



Numerical simulation and optimized design of rhombic micromixers

Jingzhi Cao¹ · Xueye Chen¹ · Xuyao Huo²

Received: 5 April 2022 / Revised: 16 August 2022 / Accepted: 26 September 2022 / Published online: 3 February 2023
© The Author(s) under exclusive licence to Associação Brasileira de Engenharia Química 2023

Abstract

In this paper, we used rhombic units to design micromixers. The influence of rhombic angles, width ratios, and the shapes of internal microchannels on mixing performance were studied. The simulation results were calculated in the range of Reynolds number (Re) 0.5 to 100. We mainly studied the mixing performance of rhombic micromixer from three aspects, including mixing efficiency, pressure drop, and fluid behavior in the microchannels. We used COMSOL Multiphysics 5.2a to simulate and calculate. The final optimized micromixer had a high mixing efficiency of more than 91.9% at all flow velocities.

Keywords Mixing efficiency · Rhombic angles · Width ratios · Chaotic convection

Introduction

The fluid in microscale is called microfluidic, and the manipulation of microfluids characterized by laminar flow is called microfluidic technology (Brouzes et al. 2009; Beebe et al. 2002; Volpatti and Yetisen 2014). Microfluidic chip technology is a technique for manipulating microfluids on a micron or even a millimetre scale. It has the ability to shrink the basic laboratory functions such as biology and chemistry to a small chip (Wu et al. 2004; Nisisako and Torii 2008). Microfluidic chip has the advantages of high efficiency, miniaturization and high integration (Flachsbart et al. 2006). Micromixer is an important part of the microfluidic chip (Hessel et al. 2005; Nguyen and Wu 2004; Yang et al. 2001). Micromixers are used in many fields of Biochemistry, such as nucleic acid synthesis or sequencing (Cheng et al. 2019), DNA purification (Fan et al. 2013), medical hygiene monitoring in combination with smart phones, and polymerase chain reaction (Arockiam et al. 2021). Microfluidic mixers have the additional advantage of reducing reaction time, such as reducing culture time for bead-based ELISA measurements (Arockiam et al. 2021).

Micromixer can be divided into active micromixer and passive micromixer according to the working principle. Active micromixer requires external energy to facilitate the mixing between different fluids (Khatavkar et al. 2007; Yu et al. 2012; Branch et al. 2011). It mainly relies on sound fields, magnetic fields, electric fields and other external energy sources to perturb the fluid and achieve mixing. For example, Daniel Ahmed et al. designed a bubble-based microfluidic structure for fast and uniform mixing. Driven by sound, the film of captured bubbles begins to oscillate. Bubble oscillation causes microbeam phenomena, i.e., strong pressure and velocity fluctuations in large liquids, which result in fast and uniform mixing of two parallel flow fluids (Ahmed et al. 2009). Wang et al. designed the micromixer by utilizing the mixing enhancement caused by alternate driving of magnetic particles suspended in the fluid. The influence of magnetic drive force, switching frequency and channel transverse dimension on the micromixer was studied (Wang et al. 2008). Michele Campisi et al. had made the device highly integrated on chip lab platforms due to low-voltage power supplies, small sizes and the possibility of manufacturing it using standard lithography technology (Campisi et al. 2009). However, the addition of active mixing into microfluids requires external equipment, complex manufacturing, heat generation and significant power requirements. The mixing time and mixing distance of active micromixers are short, but it is not easy to make due to its external energy fields. Passive micromixers promote fluid mixing by changing their geometries to change the flow trajectory of the fluids (Liu et al. 2005; Hong et al. 2001;

✉ Xueye Chen
xueye_chen@126.com

¹ College of Transportation, Ludong University,
Yantai 264025, Shandong, China

² Faculty of Mechanical Engineering and Automation,
Liaoning University of Technology, Jinzhou 121001,
Liaoning, China

Bhagat et al. 2007; Camesasca et al. 2006). For example, Park et al. enhanced mixing efficiency by adding an embedded barrier structure inside the microchannel (Park et al. 2009). Yan Du et al. obtained the optimal mixer structure by comparing the dynamic micromixing performance of the skewed slot micromixer with that of the staggered herringbone micromixer (Du et al. 2010). The Tesla structure used by Shakhawat Hossain et al. also provides a new idea for the development of passive micromixers (Treise et al. 2005). Therefore, passive micromixers that enhance mixing by modifying microchannel geometries have been widely developed because of their advantages of simplicity of fabrication and ease of integration with microfluidic systems.

Rhombus is a structure of division and convergence. The rhombic units were used to the design of micromixers which can improve the time of contact between fluids and produced chaotic convection in the microchannels. Our previous work was to design a two-dimensional rhombic passive micromixer and study the influence of rhombic angles and width ratios on mixing performance (Xu et al. 2018). Numerical simulation based on fluid dynamics has been proved to be credible for flow structures, species concentration and mixing performance (Chen and Li 2017; Chen et al. 2016; Shi et al. 2018a, 2018b). In this paper, we designed a three-dimensional rhombic micromixer, and we made innovations based on the previous research. The 60° and 90° rhombic micromixers were optimized in different ways. The optimized micromixer had high mixing efficiency in the range of Re 0.5 to 100. Hossain et al. did a numerical investigation on mixing and flow structures in microchannels with different geometries (Hossain et al. 2009). The mixing efficiency and pressure drop of the micromixer were analyzed in a wide range of Res. Chung et al. designed a planar

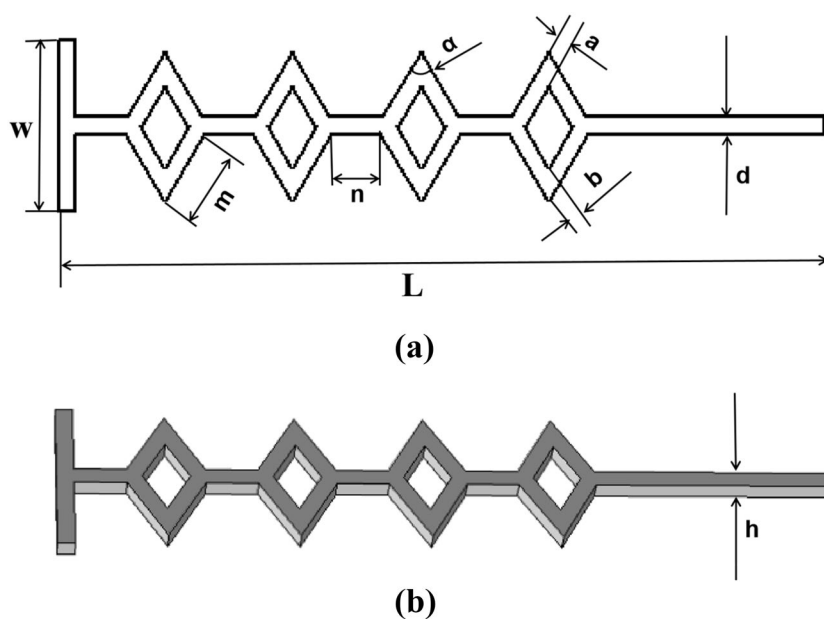
micromixer with rhombic microchannels, smaller turning angle, the higher Res and increasing number of rhombus will result in better fluid mixing (Chung and Shih 2007). Ansari et al. designed planar split and recombine micromixers with asymmetric sub-channels, the effect of the width and shape of the split channel on the mixing efficiency was studied (Ansari and Kim 2010).

In this paper, we mainly studied three geometric parameters which influenced the mixing performance of the micromixers. First, we studied the influence of rhombic angles on the mixing efficiency and pressure drop of the micromixers. Next, we optimized the 60° and 90° rhombic micromixers. The 90° rhombic micromixer was optimized by changing the shapes of the internal microchannel. The rhombic micromixer with circular internal microchannel has the highest mixing efficiency of more than 91.9% in the range of Re 0.5 to 100. Finally, the 60° rhombic micromixer is optimized by changing the microchannel width ratios. The 60° rhombic micromixer with width ratios of 1:2, 1:3, and 1:4 had a high mixing efficiency of more than 90% in the range of Re 10 to 100.

Micromixer designs

In this paper, we design the micromixer with the combination of rhombic microchannels and straight microchannels. Figure 1a shows the plane geometry of the rhombic micromixer. We design four rhombic micromixers with different rhombic angles including 30°, 45°, 60° and 90°. The influence of the microchannel width ratios of the micromixers on mixing efficiency are also studied, so we design four different width ratios of 1:1, 1:2, 1:3 and 1:4. The design of

Fig. 1 The sizes of the rhombic micromixer (a) $L = 4.5$ mm, $w = 1$ mm, $m = 0.45$ mm, $n = 0.3$ mm, $\alpha = 30^\circ, 45^\circ, 60^\circ, 90^\circ$ a:b = 1:1, 1:2, 1:3, 1:4 $d = 0.1$ mm (b) $h = 0.1$ mm



the width ratios are alternated in the rhombic micromixer. In order to further improve the mixing efficiency of the 90° rhombic micromixer, we innovatively change the internal microchannel shapes of the micromixer. We design the square and circle internal microchannels, and made a comparative analysis of their mixing performance.

Theoretical background

Navier–Stokes equation and continuity equation are used for the fluid dynamic analysis:

$$\rho \frac{\partial u}{\partial t} + \rho(u \cdot \nabla)u + \nabla P - \eta \nabla^2 u = 0 \quad (1)$$

$$\nabla \cdot u = 0 \quad (2)$$

where u is velocity vector, ρ the fluid density, t the time, η the dynamic viscosity and p is the pressure.

Convection–diffusion equation can be used to analyze the basic mixing phenomenon for the concentration:

$$\frac{\partial c}{\partial t} + (u \cdot \nabla)c = D \nabla^2 c \quad (3)$$

where, c is the species concentration and D is the diffusion coefficient.

The mixing efficiency of fluid makes us more intuitive to understand the mixing performance of fluid. The equation is as follows:

$$M = 1 - \sqrt{\frac{1}{N} \sum_{i=1}^N \left(\frac{c_i - \bar{c}}{\bar{c}} \right)^2} \quad (4)$$

where, N is the total number of sampling points, c_i the standard concentration and \bar{c} is expected standard concentration, respectively. Mixing efficiency ranges from 0 (0%, not mixing) to 1 (100%, full mixed).

Reynolds number (Re) is a important parameter for analyzing the mixing performance of fluid. The equation is as follows:

$$Re = \frac{\rho D_h U}{\mu} \quad (5)$$

where U is the average velocity of the fluid, ρ the fluid density, D_h the hydraulic diameter of the cross-section, μ is he dynamic viscosity of fluid.

In this paper, the simulation results are calculated by COMSOL Multiphysics 5.2a. The simulation environment is set to dilute material transfer and steady incompressible flows. The mixing performance of micromixers are analyzed in the range of Re 0.5 to 100. The materials used in this simulation is water and the initial concentration

conditions of the fluid are set to be $C_1 = 1$ mol/L and $C_2 = 0$ mol/L. The boundary condition of the two inlets of the micromixer is set to a fixed-velocity and the pressure of the outlet is set to be 0/pa. A reasonable grid selection is important to ensure the correctness of the results and reduce the computation time. The variance distribution of the quality scores along the channel is evaluated for the nodes with different groups to perform the grid independence test (Lv et al. 2022). Five structured grid systems are tested with a number of nodes from 49,561 to 608,855 varies as shown in Fig. 2. Because the larger the number of grid units, the slower the computer simulation will affect our computing costs, we choose a grid with a small number of grid units as the best grid partition while ensuring data accuracy. As shown in Fig. 2, we observe how the mixing efficiency varies with the number of grids. We find that the lower the number of grids, the higher the mixing efficiency, which indicates that the results are inaccurate, and as the number of grids increases, the mixing efficiency decreases and approaches the optimal number of grids. When the number of grids is 418,695, the mixing efficiency tends to reach a stable value. Even with the increasing number of grids, the mixing efficiency does not change much and the errors are within our acceptable range. More grids will slow down the simulation, so we choose 418,695 as the best grid division. The domain elements of its complete grid are counted as follows: the number of units is 418,695 and the minimum unit mass is 0.1059. The average grid quality is 0.652. The unit area ratio is 0.001359. The grid volume is 0.2922mm³. The mesh vertices of all elements are 85,472, the tetrahedrons are 209,477, the pyramids are 59,260, the triangles are 30,974, the quadrangles are 120 and the edge units are 2438. Figure 3 shows part of the grid system of the 60° rhombic micromixer.

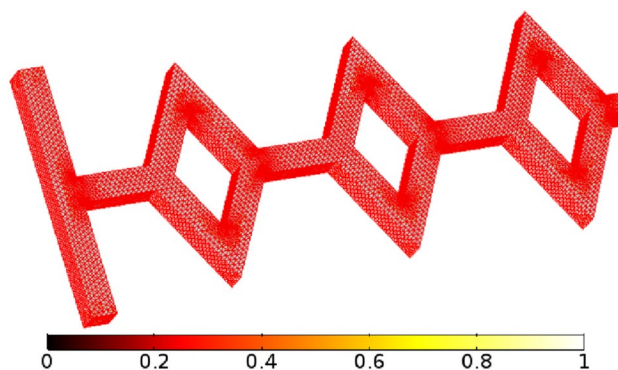


Fig. 2 The grid system of the 60° rhombic micromixer with 418,695 elements

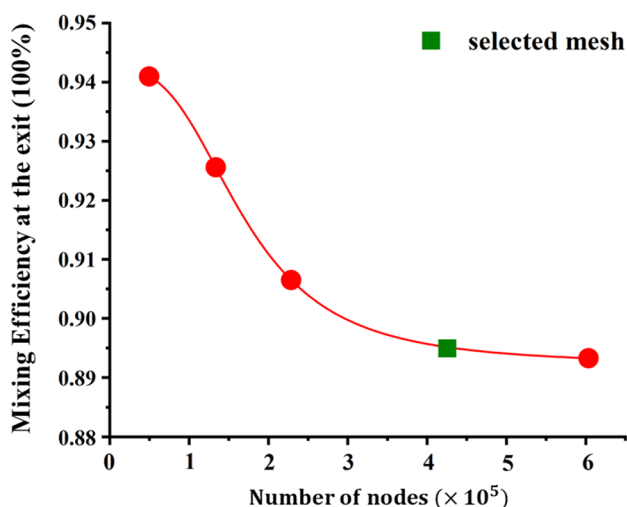


Fig. 3 Mesh refinement test for mixing efficiency at the exit at $Re = 1$

Results and discussions

The influence of rhombic angles on mixing efficiency and pressure drop

In passive rhombic micromixer, the rhombus angles have a great influence on mixing performance. The mixing performance of 30° , 45° , 60° , and 90° rhombic micromixers are compared by numerical simulation results. Figure 4 shows the simulation results of concentration of rhombic micromixers with different angles at $Re = 5$. The color legend indicates the range of concentration distribution. The more uniform the color of the fluid at the outlet of the microchannel, the higher the efficiency of the micromixer at this velocity. The mixing efficiency curves of the micromixer can more

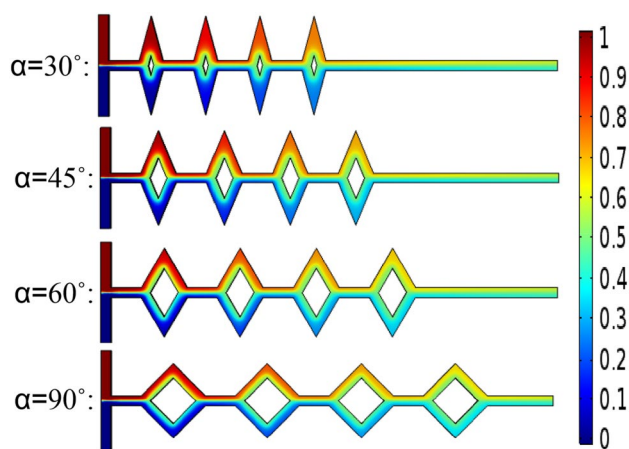


Fig. 4 The concentration results of rhombic micromixers with different angles at $Re = 5$

intuitively show us the mixing performance of the micromixer at different velocities. Figure 5 shows the mixing efficiency curves of rhombic micromixers with different rhombic angles. The simulation results are measured at $Re = 0.5, 1, 5, 10, 50,$ and 100 . The mixing efficiency curves decrease first and then increase with the increase of flow velocities. All the rhombic micromixers with different angles have the lowest mixing efficiency at $Re = 5$. The rhombic micromixer with $\alpha = 90^\circ$ has the lowest mixing efficiency of 84.9% in all the micromixers. The 90° rhombic micromixer always has the lowest mixing efficiency than the micromixers with other angles at all velocities. When Re is in the range of 0.5 to 5, the mixing efficiency of $30^\circ, 45^\circ,$ and 60° rhombic micromixers have almost the same values. In this range of velocities, there is no obvious chaotic phenomenon within the microchannels, and the fluid mainly depends on molecular diffusion to improve the mixing efficiency. When Re is within the range of 5 to 10, the mixing efficiency increases with increase of velocities, and the range of changes in mixing efficiency of all micromixers is approximately the same. In range of Re 10 to 100, the mixing efficiency of all micromixers has increased dramatically. The micromixer with the fastest increase in mixing efficiency is the 30° rhombic micromixer, and its mixing efficiency in this velocity range is higher than other micromixers. On the whole, the range of mixing efficiency of rhombic micromixers with angles of 30° to 60° is generally the same in the low velocity range. However, the micromixers with smaller rhombic angles have the higher mixing efficiency than other micromixers in the range of high velocities.

The 30° rhombic micromixer has the highest mixing efficiency when the flow velocity is high, but the mixing efficiency is low when the flow velocity is low. We analyze the fluid flow trajectory in the transverse section of the micromixer to illustrate the cause of this phenomenon. Figure 6

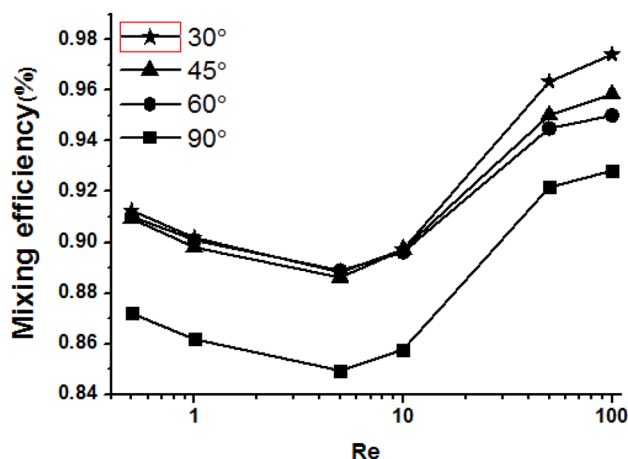


Fig. 5 The mixing efficiency of rhombic micromixers with different angles at different Res

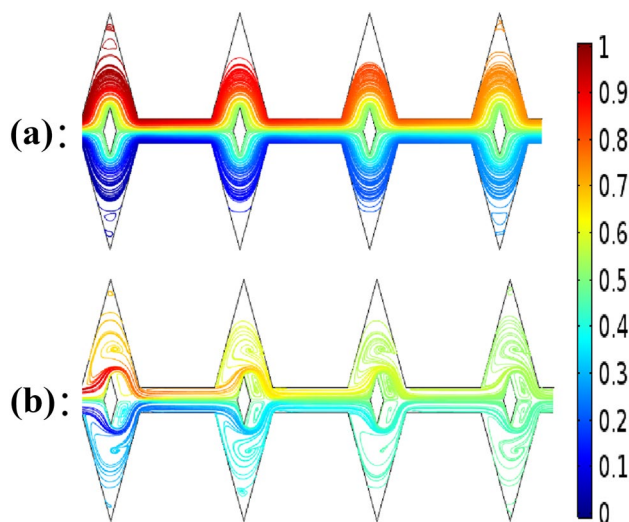


Fig. 6 The velocity field inside the microchannel of the 30° rhombic micromixer at $Re=1$ and 100 (a) $Re=1$, $v=0.01$ m/s (b) $Re=100$, $v=1$ m/s

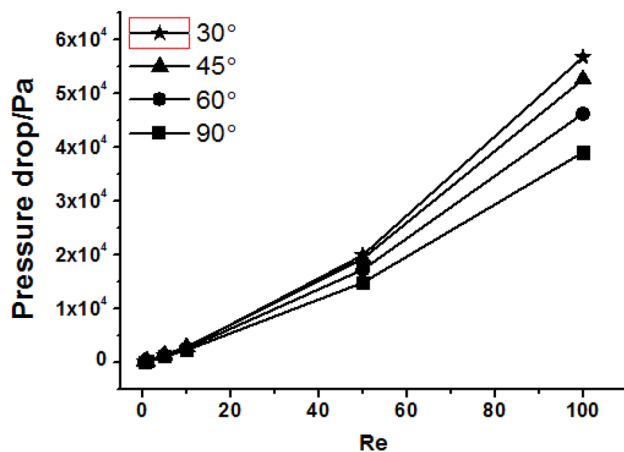


Fig. 7 The pressure drop of micromixers with different rhombic angles

shows the flow trajectory of velocity field inside the microchannel of 30° rhombic micromixer. As the results show, the chaotic convection occurs only at the corner of the rhombic microchannel when the fluid velocity is low. When the fluid velocity reach 1 m/s, it is obvious that a large area of chaotic convection appear inside microchannel.

Pressure drop variation is another important reference for comparing the mixing performance of micromixers. A micromixer with a small range of pressure drop can ensure that the micromixer will not be crushed during the manufacture. Figure 7 shows the simulation results of rhombic micromixers with different angles on pressure drop. The pressure drop are measured in the range of Re 0.5 to 100. As the results show, the pressure drop increases with the

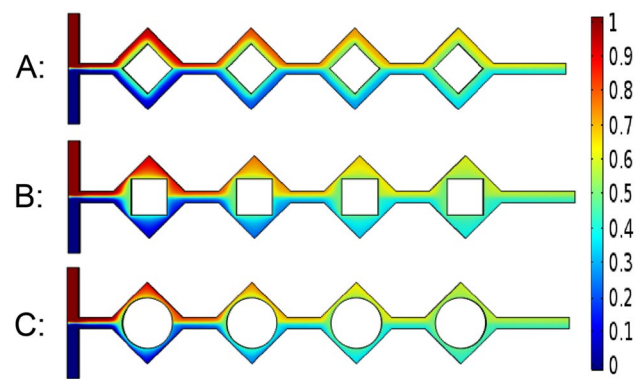


Fig. 8 The concentration results of rhombic micromixers with different internal microchannels at $Re=5$

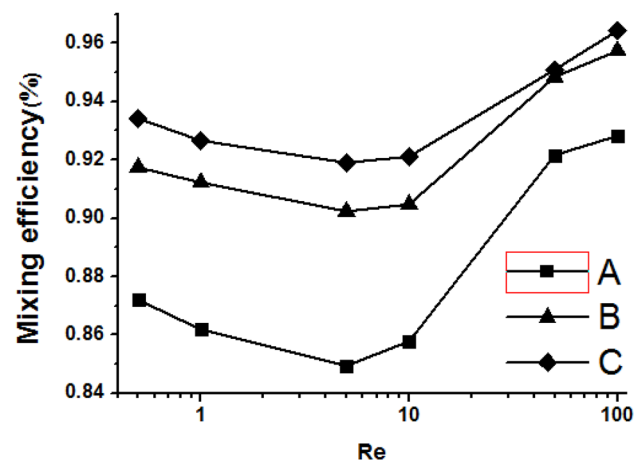


Fig. 9 The mixing efficiency of 90° rhombic micromixers with different internal channels

increase of flow velocities. The 90° rhombic micromixer has the lowest mixing efficiency, but it also has the most stable pressure drop.

The influence of internal microchannel shape of 90° rhombic micromixers on mixing efficiency and pressure drop

From the above discussion, we know that the 90° rhombic micromixer has the lowest mixing efficiency than the other micromixers. We further improve the mixing efficiency of the 90° rhombic micromixer by changing the internal microchannel shapes. Figure 8 shows the simulation results of concentration of rhombic micromixers with different internal microchannels at $Re=5$. The diameter of the circular internal microchannel is equal to the diagonal length of the square internal microchannel. Figure 9 shows the simulate results of rhombic micromixers with different internal microchannel shapes on mixing efficiency in the

range of Re 0.5 to 100. As shown in the results, the mixing efficiency of the rhombic micromixers with square and circular internal microchannel shapes was higher than that of the original design. The rhombic micromixer with circular internal microchannel has the highest mixing efficiency of more than 91.9% in the range of Re 0.5 to 100. All the rhombic micromixers have the lowest mixing efficiency when $Re = 5$. When Re is within the range of 0.5 to 5, the mixing efficiency decreases as the flow velocity increases. When the fluid flows in the microchannel at low velocity, it mainly depends on molecular diffusion to improve mixing efficiency. The time of the molecular diffusion is shortened with the increase of fluid velocities, thus the mixing efficiency is gradually reduced. When Re is in the range of 5 to 10, the chaotic convection phenomenon in the microchannel is gradually strengthened, so the mixing efficiency has a trend of increasing. When Re is in the range of 10 to 100, the mixing efficiency of micromixers rises sharply. The 90° rhombic micromixer with circle internal microchannel has a mixing efficiency of 96.4% at $Re = 100$.

Figure 10 shows the pressure drop of micromixers with different internal microchannel shapes, the simulation results are measured at $Re = 0.5, 1, 5, 10, 50,$ and 100 . As the results show, the pressure drop rises gradually as the fluid velocities increase. Although the mixing efficiency of the 90° micromixer is the lowest, it also has the most stable pressure drop. The mixing efficiency of the micromixer with a circular internal microchannel is the highest, but its pressure drop difference is also the largest.

The influence of width ratios of 60° rhombic micromixers on mixing efficiency and pressure drop

The microchannel width of the micromixer has a great influence on the mixing performance. We design a 60°

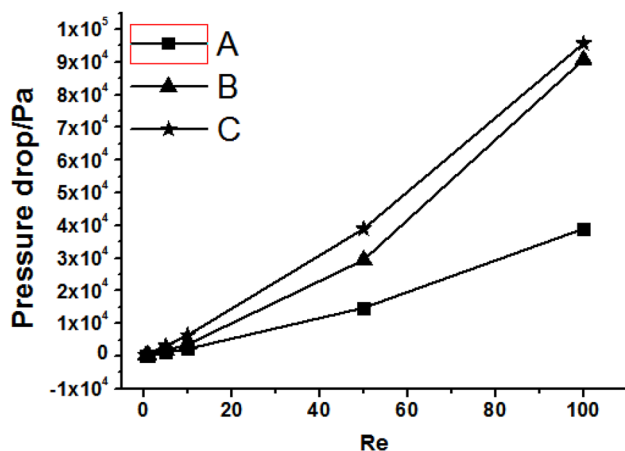


Fig. 10 The pressure drop of 90° micromixers with different internal microchannel shapes

rhombic micromixer with different width ratios and compared the mixing efficiency and pressure drop of the micromixers. Figure 11 shows the simulation results of 60° rhombic micromixers with different width ratios on concentration at $Re = 5$. We analyze four kinds of rhombic micromixers with different width ratios, included 1:1, 1:2, 1:3, and 1:4. The mixing efficiency curves allow us to compare the mixing performance more clearly. Figure 12 shows the simulation results of rhombic micromixers with different width ratios on mixing efficiency. As shown in the results, the mixing efficiency of all micromixers decreases first and then increases with the increase of flow velocities. All micromixers have the lowest mixing efficiency at $Re = 5$. In the range of Re 0.5 to 5, the mixing efficiency of all micromixers decreases, but the range of variation is small. The 60° rhombic micromixer with width ratio 1:1 has the highest mixing efficiency in the range of Re

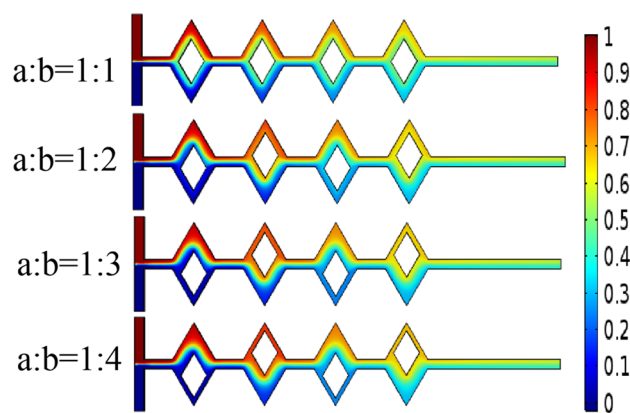


Fig. 11 The concentration results of 60° rhombic micromixers with different width ratios

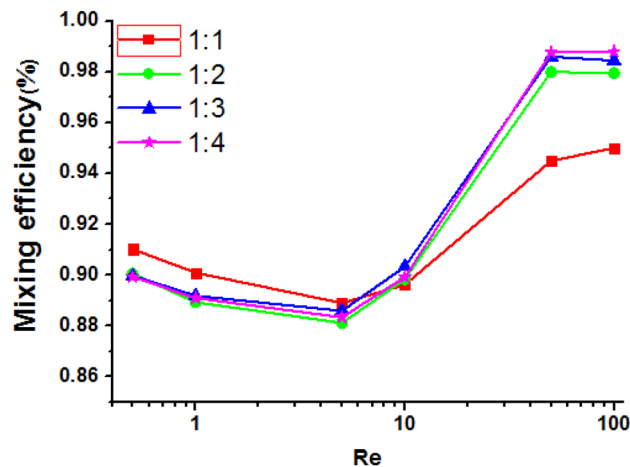


Fig. 12 The mixing efficiency of 60° rhombic micromixers with different width ratios

0.5 to 5 than the micromixers with width ratios 1:2, 1:3, and 1:4. In the range of Re 5 to 10, the mixing efficiency of all micromixers increases, but not by much. Among them, the mixing efficiency of rhombic micromixer with a width ratio of 1:1 has the smallest increase. In the range of Re 10 to 50, the mixing efficiency of all micromixers is greatly increase. The rhombic micromixers with width ratios of 1:2, 1:3, and 1:4 have a better mixing efficiency than the micromixer with ratio of 1:1. The micromixer with width ratio of 1:4 has a high mixing efficiency of 98.7% at $Re = 50$. The mixing efficiency of the micromixer continues to increase and tends to stabilize. In general, the rhombic micromixer with width ratio of 1:1 has a better mixing performance than the micromixer with width ratios of 1:2, 1:3, and 1:4 at low velocities. The micromixer width ratios of 1:2, 1:3, and 1:4 have a better mixing performance than the micromixer with width ratio of 1:1 at high velocities. Changing the microchannel width ratios of micromixers can greatly improve the mixing efficiency at high flow velocities. In the range of Re 50 to 100, the 60° micromixers with width ratios of 1:3 and 1:4 achieve almost complete mixing.

Through the analysis of the above mixing efficiency curves, the mixing efficiency of 60° rhombic micromixer with width ratio of 1:4 has a high mixing efficiency at high flow velocities. When $Re = 100$, the mixing efficiency of the 60° rhombic micromixer with width ratio of 1:4 reaches about 98.7%, which is almost close to complete mixing. Figure 13 shows the concentration changes inside the microchannel of 60° rhombic micromixer with width ratio of 1:4 at $Re = 100$. The color legend represents the concentration range. As the results show, the two fluids with different concentrations flow from the two inlets, and eventually achieve almost complete mixing. The color change of the concentration on the cross-section gradually becomes uniform. Figure 14 shows the pressure drop of 60° rhombic micromixer with different width ratios. The pressure drop of all micromixers increases as the flow velocity increases. The pressure drop are measured at $Re = 0.5, 1, 5, 10, 50,$ and 100 . In the range of Re 0.5 to 50, the range and trend of all micromixers on pressure drop are consistent. In the range of Re 50 to 100, the pressure drop ranges of the micromixers began to vary. However, it is obvious that the pressure drop difference of all micromixers is very small at high Re s.

The influence of microchannel shape in rhombic micromixer on mixing cost

The mixing cost (MC) has also been used as a literature to evaluate the performance parameters of micromixers. Lower MC values indicate better micromixer performance. The expression of MC can be written as follows:

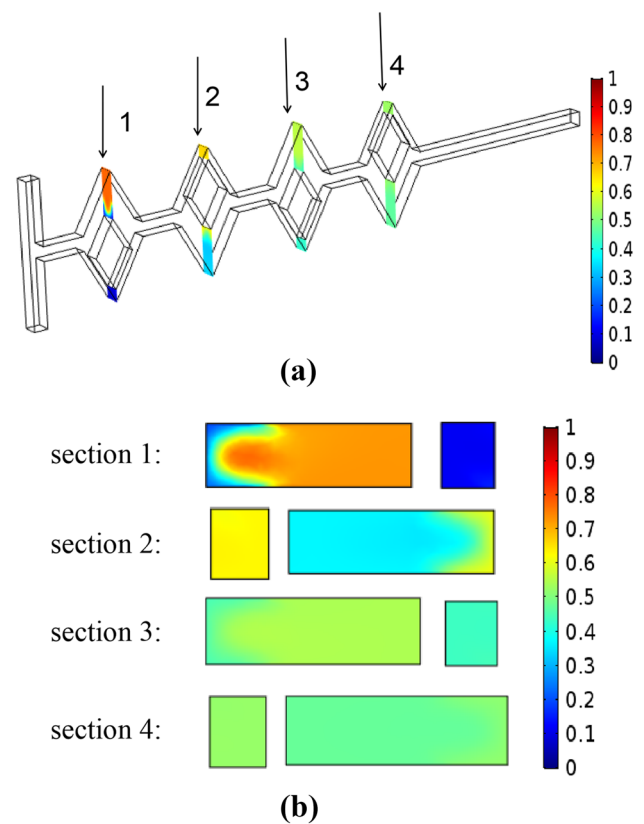


Fig. 13 The change of concentration in cross-section of the 60° rhombic micromixer with width ratio of 1:4 at $Re = 100$

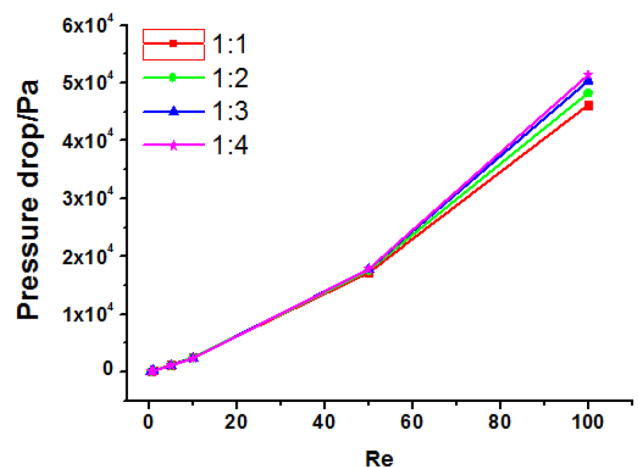


Fig. 14 The pressure drop of 60° rhombic micromixers with different width ratios

$$mc = \frac{\Delta p}{M} \quad (6)$$

implying that the units for MC are Pa/%. As we can see from Table 1, these values are usually obtained from very

Table 1 Comparison of mixing cost of the micromixer under various architectures at five Reynolds numbers

Parameters	mc (Pa/%)					
	Re = 0.5	Re = 1.0	Re = 5.0	Re = 10	Re = 50	Re = 100
$\alpha = 30^\circ$	1.397	2.831	14.626	30.027	206.408	581.829
$\alpha = 45^\circ$	1.473	2.988	15.383	31.331	202.661	548.162
$\alpha = 60^\circ$	1.349	2.729	14.051	28.712	182.014	486.015
$\alpha = 90^\circ$	1.232	2.496	12.859	26.188	160.339	420.081
A	1.858	3.742	19.277	40.058	310.332	948.306
B	1.232	2.496	12.859	26.188	160.339	420.081
C	3.349	6.758	34.350	69.676	410.161	992.339
a : b = 1 : 1	1.349	2.719	14.052	28.951	182.012	486.235
a : b = 1 : 2	1.313	2.663	13.682	27.757	179.692	493.015
a : b = 1 : 3	1.263	2.553	13.095	26.649	180.723	511.712
a : b = 1 : 4	1.234	2.495	12.805	26.105	180.802	522.809

complex micromixer designs and are very large. We summarized all the rhombic micromixers with different structures and compared the mixing costs of these micromixers. The results show that the mixing cost of all the micromixers increases to some extent with the increase of flow rate. When $Re = 0.5$, the mixing cost of all the micromixers is the lowest because the pressure drop in the microchannel is the lowest. In the range of $Re = 0.5$ to $Re = 1.0$, the change of mixing cost is mainly influenced by flow rate, and the value of mixing cost is related to the value of Reynolds number. In the range of $Re = 10$ to 100 , the mixing cost of all the micromixers has been greatly increased, mainly because when the Reynolds number is large enough, the pressure drop is large enough to be significantly affected by the pressure drop.

Conclusion

In this paper, we studied the optimization designs and numerical simulations of the three-dimensional rhombic micromixers. We analyzed the mixing performance of the micromixers based on mixing efficiency, pressure drop, and the fluid flow in microchannels. First, we designed the 30° , 45° , 60° and 90° rhombic micromixers, and compared the influence of rhombic angles on mixing performance of the micromixers. The 30° rhombic micromixers had a high mixing efficiency at high Res. Secondly, we optimized the design of the 90° rhombic micromixer. We changed the internal microchannel shapes of micromixers. The 90° rhombic micromixer with circular internal microchannel had the highest mixing efficiency of more than 91.9% in the range of Re 0.5 to 100. Finally, we improved the mixing efficiency of 60° rhombic micromixer by changing the microchannel width ratios. The optimized 60° rhombic micromixer with a width ratio of 1:4 achieved almost complete mixing at high velocities and had a lower pressure drop change. The simulation results show that the optimization designs of rhombic

micromixers can be widely used in biological engineering and chemical engineering.

Acknowledgements This work was supported by Young Taishan Scholars Program of Shandong Province of China (tsqn202103091), Special Supporting Funds for Leading Talents at or Above the Provincial Level in Yantai City.

Declarations

Conflict of interest The authors declare no conflicts of interest.

References

- Ahmed D, Mao X, Juluri BK et al (2009) A fast microfluidic mixer based on acoustically driven sidewall-trapped microbubbles[J]. *Microfluid Nanofluid* 7(5):727–731
- Ansari MA, Kim KY (2010) Mixing performance of unbalanced split and recombine micromixers with circular and rhombic sub-channels[J]. *Chem Eng J* 162(2):760–776
- Arockiam S, Cheng YH, Armenante PM et al (2021) Experimental determination and computational prediction of the mixing efficiency of a simple, continuous, serpentine-channel microdevice[J]. *Chem Eng Res Des* 167:303–317
- Beebe D, Wheeler M, Zeringue H et al (2002) Microfluidic technology for assisted reproduction[J]. *Theriogenology* 57(1):125–135
- Bhagat AAS, Peterson ETK, Papautsky I (2007) A passive planar micromixer with obstructions for mixing at low Reynolds numbers[J]. *J Micromech Microeng* 17(5):1017
- Branch DW, Meyer GD, Craighead HG (2011) Active micromixer using surface acoustic wave streaming: U.S. Patent 7,942,568[P]. 2011–5–17.
- Brouzes E, Medkova M, Savenelli N et al (2009) Droplet microfluidic technology for single-cell high-throughput screening[J]. *Proc Natl Acad Sci* 106(34):14195–14200
- Camasasca M, Kaufman M, Manas-Zloczower I (2006) Staggered passive micromixers with fractal surface patterning[J]. *J Micromech Microeng* 16(11):2298
- Campisi M, Accoto D, Damiani F et al (2009) A soft-lithographed chaotic electrokinetic micromixer for efficient chemical reactions in lab-on-chips[J]. *Journal of Micro-Nano Mechatronics* 5(3):69–76

- Chen X, Li T (2017) A novel passive micromixer designed by applying an optimization algorithm to the zigzag microchannel. *Chem Eng J* 313:1406–1414
- Chen X, Shen J, Zhou M (2016) Rapid fabrication of a four-layer PMMA-based microfluidic chip using CO₂-laser micromachining and thermal bonding. *J Micromech Microeng* 26(10):107001
- Cheng YH, Moura PAR, Zhenglong L et al (2019) Effect of electrode configuration on the sensitivity of nucleic acid detection in a non-planar, flow-through, porous interdigitated electrode[J]. *Biomicrofluidics* 13(6):064118
- Chung CK, Shih TR (2007) A rhombic micromixer with asymmetrical flow for enhancing mixing[J]. *J Micromech Microeng* 17(12):2495
- Du Y, Zhang Z, Yim CH et al (2010) Evaluation of floor-grooved micromixers using concentration-channel length profiles[J]. *Micromachines* 1(1):19–33
- Fan A, Byrnes S, Klapperich C (2013) Purification of DNA/RNA in a microfluidic device[M]//*Microfluidic Diagnostics*. Humana Press, Totowa, NJ, pp 403–411
- Flachsbarth BR, Wong K, Iannacone JM et al (2006) Design and fabrication of a multilayered polymer microfluidic chip with nanofluidic interconnects via adhesive contact printing[J]. *Lab Chip* 6(5):667–674
- Hessel V, Löwe H, Schönfeld F (2005) Micromixers—a review on passive and active mixing principles[J]. *Chem Eng Sci* 60(8–9):2479–2501
- Hong CC, Choi JW, Ahn CH (2001) A novel in-plane passive micromixer using Coanda effect[C]//*Micro Total Analysis Systems*. Springer, Dordrecht 2001:31–33
- Hossain S, Ansari MA, Kim KY (2009) Evaluation of the mixing performance of three passive micromixers[J]. *Chem Eng J* 150(2–3):492–501
- Khatavkar VV, Anderson PD, den Toonder JMJ et al (2007) Active micromixer based on artificial cilia[J]. *Phys Fluids* 19(8):083605
- Liu A, He F, Wang K et al (2005) Rapid method for design and fabrication of passive micromixers in microfluidic devices using a direct-printing process[J]. *Lab Chip* 5(9):974–978
- Lv H, Chen X, Wang X et al (2022) A novel study on a micromixer with Cantor fractal obstacle through grey relational analysis[J]. *Int J Heat Mass Transf* 183:122159
- Nguyen NT, Wu Z (2004) Micromixers—a review[J]. *J Micromech Microeng* 15(2):R1
- Nisisako T, Torii T (2008) Microfluidic large-scale integration on a chip for mass production of monodisperse droplets and particles[J]. *Lab Chip* 8(2):287–293
- Park JM, Seo KD, Kwon TH (2009) A chaotic micromixer using obstruction-pairs[J]. *J Micromech Microeng* 20(1):015023
- Shi YZ, Xiong S, Zhang Y et al (2018a) Sculpting nanoparticle dynamics for single-bacteria-level screening and direct binding-efficiency measurement. *Nat Commun* 9(1):815
- Shi Y, Xiong S, Chin L K, et al. Nanometer-precision linear sorting with synchronized optofluidic dual barriers. *Science advances*, 2018b, 4(1):eaa0773
- Treise I, Fortner N, Shapiro B et al (2005) Efficient energy based modeling and experimental validation of liquid filling in planar microfluidic components and networks[J]. *Lab Chip* 5(3):285–297
- Volpatti LR, Yetisen AK (2014) Commercialization of microfluidic devices[J]. *Trends Biotechnol* 32(7):347–350
- Wang Y, Zhe J, Chung BTF et al (2008) A rapid magnetic particle driven micromixer[J]. *Microfluid Nanofluid* 4(5):375–389
- Wu H, Wheeler A, Zare RN (2004) Chemical cytometry on a picoliter-scale integrated microfluidic chip[J]. *Proc Natl Acad Sci* 101(35):12809–12813
- Xu J, Chen X, Liu Y et al (2018) Numerical study on micromixers with smart-rhombic structure[J]. *Int J Mod Phys B* 32(27):1850301
- Yang Z, Matsumoto S, Goto H et al (2001) Ultrasonic micromixer for microfluidic systems[J]. *Sens Actuators, A* 93(3):266–272
- Yu S, Jeon TJ, Kim SM (2012) Active micromixer using electrokinetic effects in the micro/nanochannel junction[J]. *Chem Eng J* 197:289–294

Publisher's Note Springer Nature remains neutral with regard to jurisdictional claims in published maps and institutional affiliations.

Springer Nature or its licensor (e.g. a society or other partner) holds exclusive rights to this article under a publishing agreement with the author(s) or other rightsholder(s); author self-archiving of the accepted manuscript version of this article is solely governed by the terms of such publishing agreement and applicable law.